ADVANCED FUNCTIONAL MATERIALS

Supporting Information

for *Adv. Funct. Mater.,* DOI: 10.1002/adfm.202100431

An Instant Change of Elastic Lattice Strain during Cu_2Se Phase Transition: Origin of Abnormal Thermoelectric Properties

Hui Bai, Xianli Su, Dongwang Yang, Qingjie Zhang, Gangjian Tan, Ctirad Uher, Xinfeng Tang, and Jinsong Wu**

Supporting Information For:

An instant change of elastic lattice strain during Cu_2Se phase transition: origin of abnormal thermoelectric properties

Hui Bai[1,2†], Xianli Su[1†], Dongwang Yang[1], Qingjie Zhang[1], Gangjian Tan[1], Ctirad Uher[3], Xinfeng Tang[1*] and Jinsong Wu[1,2*]

[1]*State Key Laboratory of Advanced Technology for Materials Synthesis and Processing, Wuhan University of Technology, Wuhan 430070, China*

[2]*Nanostructure Research Center, Wuhan University of Technology, Wuhan 430070, China*

[3]*Department of Physics, University of Michigan, Ann Arbor, Michigan 48109, USA*

[†]These authors contributed equally to this work.

*Correspondence and requests for materials should be addressed to Jinsong Wu (wujs@whut.edu.cn) and Xinfeng Tang (tangxf@whut.edu.cn).

This PDF includes:

A. Figures S1 to S7

B. Videos S1 to S6

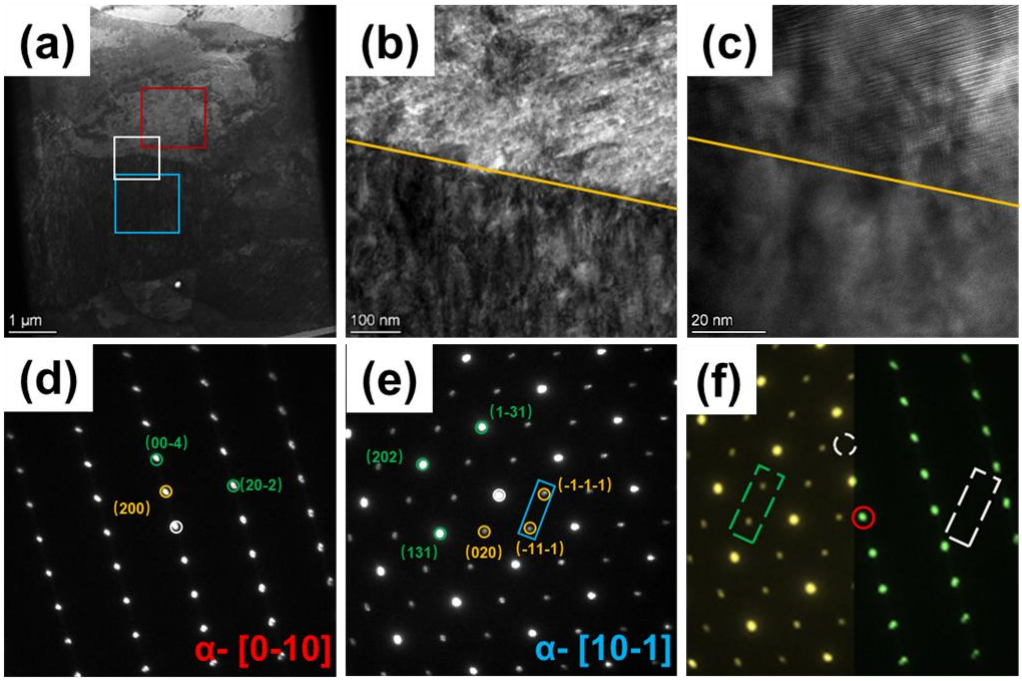

Figure S1. Characterization of Cu_2Se sample structure. TEM images (a-c) on both sides of the Cu_2Se grain boundary (yellow dashed line) under different magnifications. Selected area electron diffraction of the red area (d) and the blue area (e) in (a). Comparison of differences in the two diffractions in (f).

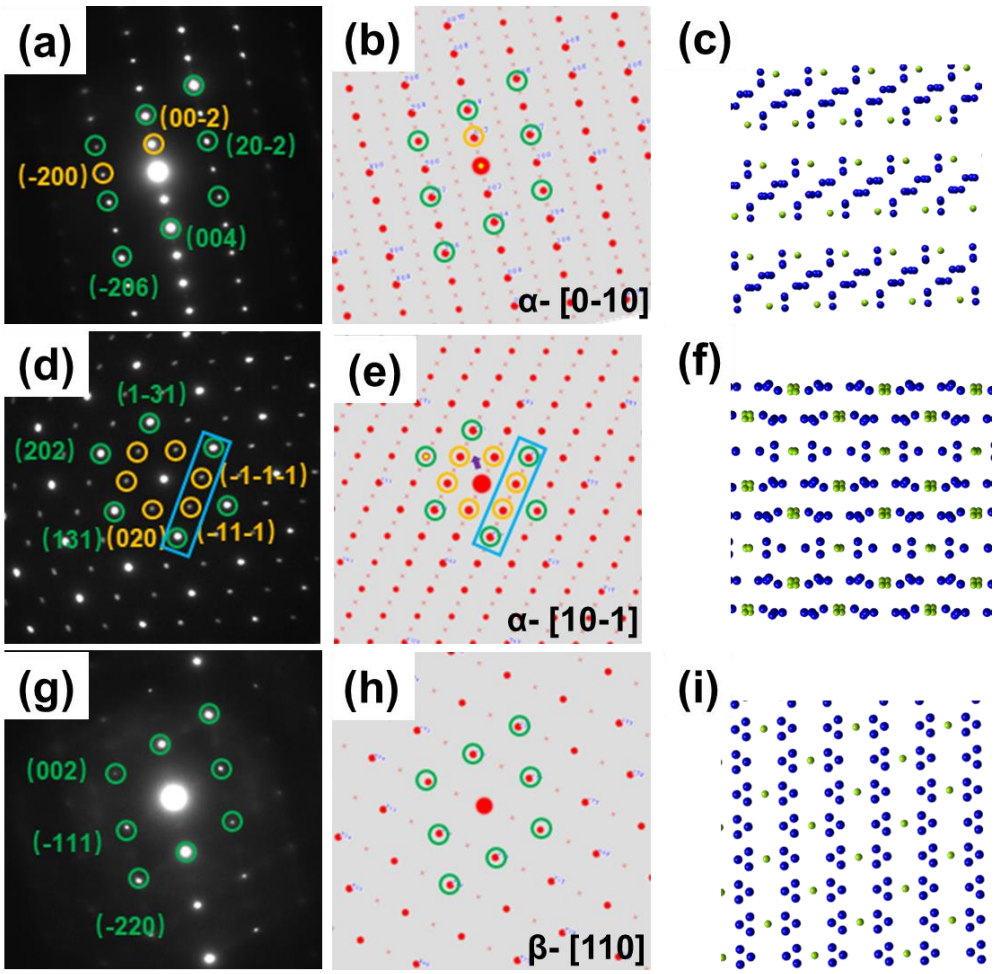

Figure S2. Structual relationships in Cu_2Se before and after phase transformation. Selected area electron diffraction (a, d, g), simulated electron diffraction (b, e, h), and structural schematic diagrams (c,e,i) of α-phase Cu_2Se along [0-10], [10-1] and β-phase Cu_2Se along [110] directions are compared, respectively.

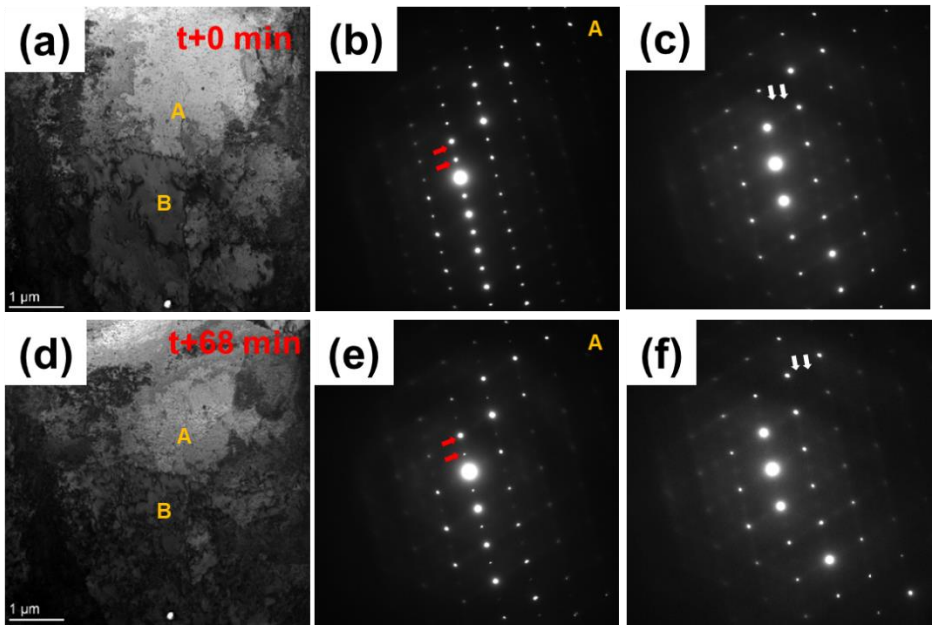

Figure S3. The Cu_2Se structure is stable at 388 K for a long time. (a,d) Low magnification TEM images at 0 min and 68 min. (b,e) Electron diffraction from the A crystal grains. (c,f) Electron diffraction from the B crystal grains.

(a)

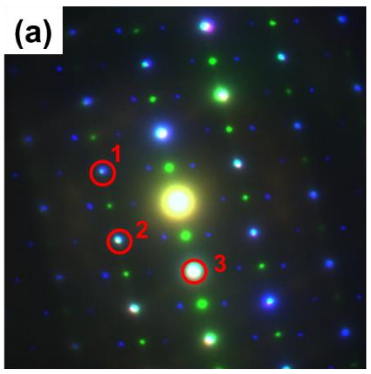

(b)

	1	2	3
	$d_{Theoretical}$ (nm)	$d_{Theoretical}$ (nm)	$d_{Theoretical}$ (nm)
α- [10-1]	(202)	(131)	(-13-1)
	0.2927	0.3367	0.3367
α- [0-10]	(-20-2)	(-202)	(004)
	0.2927	0.3375	0.3406
β- [110]	(002)	(-111)	(-11-1)
	0.2935	0.3389	0.3389

Figure S4. Contrast in the diffraction patterns of the α-Cu_2Se [10-1] domain, α-Cu_2Se [0-10] domain, and β-Cu_2Se [110].

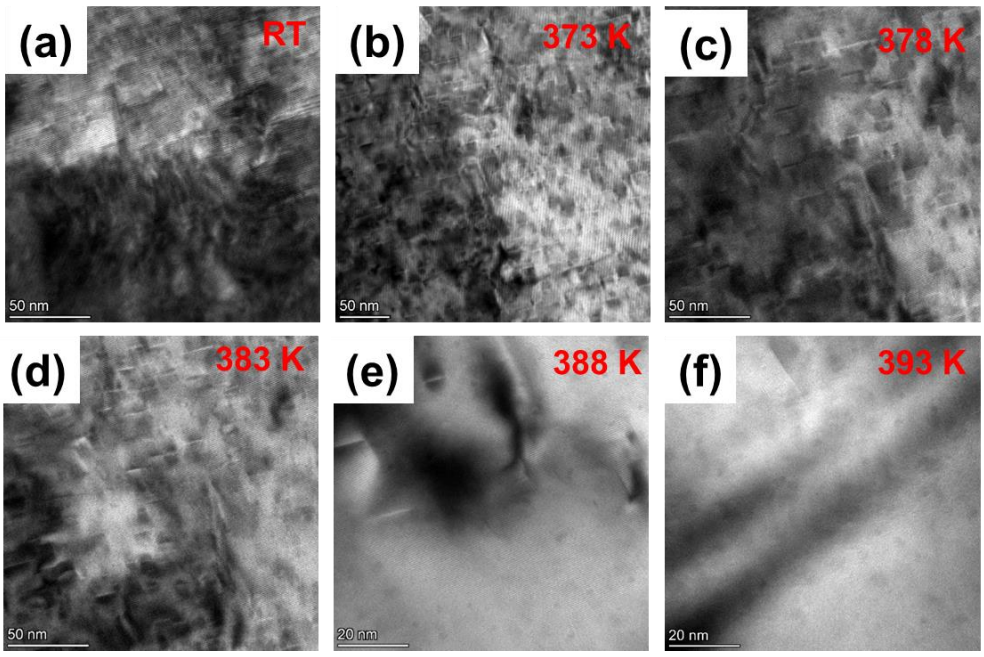

Figure S5. Dislocation changes in Cu_2Se upon *in-situ* heating at different temperatures. The temperatures are (a) RT, (b) 373 K, (c) 378 K, (d) 383 K (e) 388 K, and (f) 393 K.

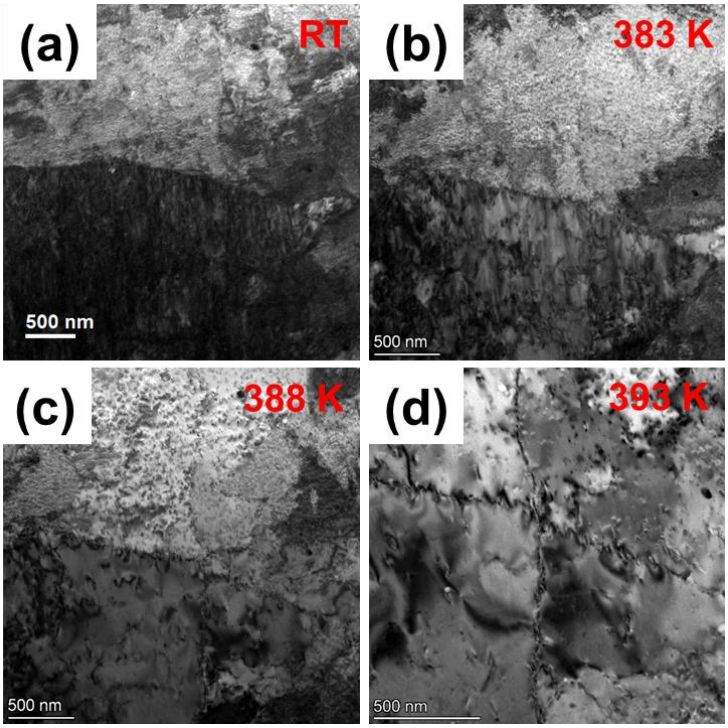

Figure S6. Low-magnification TEM images of Cu_2Se during the *in-situ* heat-induced phase transformation at different temperatures. The temperatures are (a) RT, (b) 383 K, (c) 388 K and (d) 393 K.

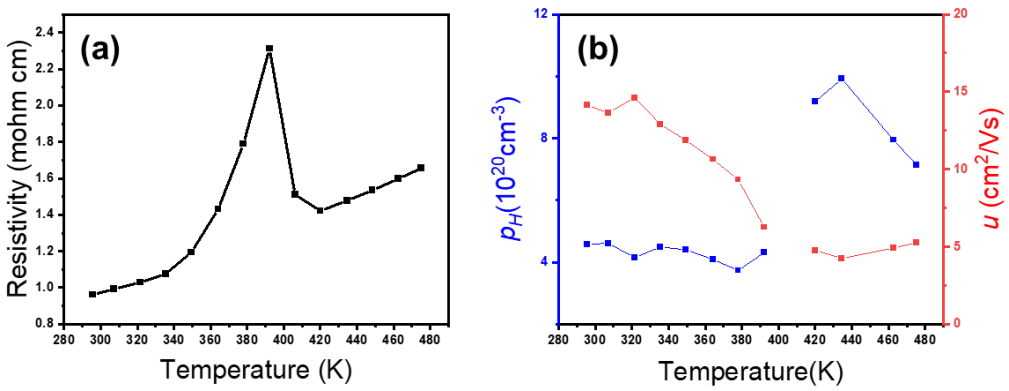

Figure S7. Thermoelectric properties of Cu_2Se as a function of temperature: (a) resistivity, (b) carrier concentration (p_H) and carrier mobility (μ).

B. Videos

Video S1. *In-situ* TEM of the Cu_2Se phase transformation by rising temperature from room temperature to ~120°C (×5 times faster than the real speed).

Video S2. *In-situ* selected area electron diffraction (SAED) patterns from α-Cu_2Se [1-21] domain to β-Cu_2Se [112], when the temparatur is raised from 100 to 150°C (×5 times faster than the real speed).

Video S3. *In-situ* SAED patterns from β-Cu_2Se [112] to α-Cu_2Se [100] domain, when the temparatur is decreased from 150 to 100°C (×5 times faster than the real speed).

Video S4. *In-situ* SAED patterns from α-Cu_2Se [100] domain to β-Cu_2Se [112], when the temparatur is raised from 100 to 150°C (×5 times faster than the real speed).

Video S5. *In-situ* SAED patterns from β-Cu_2Se [112] to α-Cu_2Se [1-21] domain, when the temparatur is decreased from 150 to 100°C (×5 times faster than the real speed).

Video S6. *In-situ* high resolution STEM of the the Cu_2Se phase transformation, when the temparatur is cycled back and forth among 110 to 115°C.